



A study on copula-based bivariate and trivariate drought assessment in Godavari River basin and the teleconnection of drought with large-scale climate indices

Soumyashree Dixit¹ · K. V. Jayakumar¹

Received: 1 November 2020 / Accepted: 16 September 2021 / Published online: 2 October 2021
© The Author(s), under exclusive licence to Springer-Verlag GmbH Austria, part of Springer Nature 2021

Abstract

The single variable-dependent drought cannot adequately define the onset and withdrawal characteristics of the droughts. A Multivariate Standardised Drought Index (MSDI) is developed in the present study, based on precipitation and soil moisture using bivariate copula function. Reconnaissance Trivariate Drought Index (RTDI) is also developed combining precipitation, soil moisture and evapotranspiration. MSDI and RTDI represent meteorological and agricultural droughts by linking the climate status in an effective way. The best fitted copulas obtained for bivariate and trivariate analyses are Frank and Student's t copulas respectively. The two drought indices are developed and tested to study the onset and withdrawal characteristics of drought and their trends. Cross-wavelet analysis (CWA) is performed to identify the substantial effect of large-scale climate anomalies on the derived drought indices. The large-scale climate factors like sea surface temperature (SST), Multivariate ENSO Index (MEI), Southern Oscillation Index (SOI), Indian Ocean Dipole (IOD) and Indian summer monsoon rainfall (ISMR) are considered in this study. ENSO, IOD and ISMR showed significant influences on the drought variability. The 3-month MSDI is significantly influenced by ISMR while SST showed a significant teleconnection with RTDI-3. The SST showed a strong influence on both 6-month MSDI and 6-month RTDI. This study is robust and reliable for future drought assessment and will provide a great platform to develop warning criteria on onset and termination of droughts.

1 Introduction

Drought is defined as a natural and anthropogenic hazard that causes a significant depletion in the water supply below the demand during a particular time span. Increasing drought events have been occurring in different parts of the world, with devastating influences on agriculture, economy and environment. Droughts are generally categorised as (i) 'meteorological drought', a prolonged time span in month or year with deficit amount of precipitation; (ii) 'agricultural drought', occurring when the soil moisture is reduced below the permanent wilting point; and (iii) 'hydrological drought', occurring when storage of water, streamflow and groundwater levels is below the required level (Mishra and

Singh, 2010). Drought can also be explained by timing (i.e. occurrence of drought in the principle season, shifting of monsoon) and the characteristics of the rainfall (intensity of rainfall, the total number of rainfall events, etc.). India is mostly an agricultural dominant country. About 68% of the total agricultural area in India is vulnerable to drought directly affecting the economy status of the country (Dutta et al., 2015). Mishra et al. (2016) reported that the drought with a return period of 542 years highly influenced the water demand in India. The northern, central-eastern, western and central regions of India are highly prone to natural extremities like floods and droughts (Kumar et al. 2021c). Hence, it is important to understand the multi-scalar and multi-dimensional drought phenomenon, especially an agricultural based country like India.

The drought indices like Standardised Precipitation Index (SPI, McKee et al. 1993), Standardised Runoff Index (SRI, Shukla and Wood, 2008) and Standardised Soil moisture Index (SSI, Hao and AghaKouchak, 2013) reflect only a specific system of drought that could be hydrological, meteorological or agricultural drought. These indices neither indicate the different climatic variable deficit nor quantify

✉ Soumyashree Dixit
dixitsoumya27@gmail.com

K. V. Jayakumar
kvj@nitw.ac.in

¹ Department of Civil Engineering, National Institute of Technology Warangal, Warangal, India

the drought condition because they depend on multiple variables (Rajsekhar et al. 2015). For example, the only variable which is used for finding the SPI is the precipitation. However, the dependency only on precipitation, neglecting the ground-related variables and evapotranspiration may narrow down the effectiveness of drought monitoring. Proper drought management requires the background knowledge of drought magnitude and occurrences based on multiple variables. To overcome the drought assessment of single-valued drought index, multiple drought indices are developed by various researchers. All forms of droughts were considered in the development of Aggregated Drought Index (ADI) by Keyantash and Dracup (2004) including all possible real-time input variables like precipitation, soil moisture, reservoir storage, streamflow and evapotranspiration and snow. Rajsekhar et al. (2015) demonstrated a kernel entropy component analysis (KECA) to construct a Multivariate Drought Index (MDI). Huang et al. (2016) developed the Multivariate Standardised Reliability and Resilience Index (MSRRI) that combined the information of Inflow-Demand Reliability Index (IDRI) and Water Storage Resilience Index (WSRI). Liu et al. (2020) evaluated the MSRRI for the Northwest China region.

Copula-based multivariate approaches have proved to be a reliable way for assessing the drought phenomenon, and these approaches are gaining significant recognition in the field of hydrology (Mishra and Singh, 2009; Gupta et al. 2020; Poonia et al. 2021). A Joint Drought Index (JDI) using copula for obtaining the joint probabilities while considering precipitation and streamflow in the State of Indiana was introduced by Kao and Govindaraju (2010). Hao and AghaKouchak (2013) used a 2-dimensional Frank copula-based Multivariate Standardised Drought Index (MSDI) to represent a drought considering both meteorological and agricultural droughts in California and North Carolina. Ma et al. (2014) computed a Composite Drought Index (CDI) using monthly precipitation, temperature and soil moisture by merging PDSI and Standardised Palmer Drought Index (SPDI) through a potential moisture departure probabilistic approach. Shah and Mishra (2020a, b) developed an Integrated Drought Index (IDI) by combining a number of drought indices using copula SPI, SSI, SRI and Standardised Groundwater Index (SGI). Copula-based Joint Drought Index (CJDI) developed by (Won et al. 2020) combines the properties of SPI and Evaporative Demand Drought Index (EDDI).

Many studies have been carried out in the past to identify the impact of climate variability with respect to the large-scale climate oscillations (Hao et al. 2018; Zhang et al., 2020; Das et al. 2020a, b; Jha et al. 2021). Furthermore, global variations in the large-scale climate oscillations have significant teleconnections with drought events (Wang and Kumar, 2015; Guo et al. 2019). So, the present study

employed a cross-wavelet analysis (CWA) method to obtain correction between large-scale climate features and drought phenomenon. The cross-correlations between ENSO events and Non-parametric Multivariate Standardised Drought Index (NMSDI) were investigated using the CWA analysis by Huang et al. (2016). The positive ENSO has substantial impact on the drought frequency in India (Shah and Mishra, 2020a, b). Kumar et al. (2021a) used CWA method to identify the association between large-scale climate oscillations with the drought characteristics focusing on groundwater over south Indian river basins. Hence, to obtain the teleconnections of large-scale climate indices with drought events, the impact of five climate signals like Southern Oscillation Index (SOI), sea surface temperature (SST), Multivariate ENSO Index (MEI), Indian Ocean Dipole (IOD) and Indian summer monsoon rainfall (ISMR) on multivariate drought is examined using the CWA method.

Shah and Mishra (2020a, b) reported that the real-time drought assessment in India has been a challenging task due to the lack of near-real-time observations. There are major difficulties in detecting the onset and withdrawal of droughts. The information regarding the drought indices are not readily available to state governments. Indian river basins are highly vulnerable to extreme calamities like drought (Pathak and Dodamoni 2020; Poonia et al. 2021; Kumar et al. 2021b). This study considered the Godavari River basin, the second largest river basin in India and flowing across the states of Maharashtra, Madhya Pradesh, Telangana, Andhra Pradesh, Karnataka, Odisha and Chhattisgarh. This basin is highly vulnerable to drought (Dixit et al. 2021). Furthermore, the large-scale climate indicators impacting the multi-variate drought phenomenon have rarely been explored on a river basin scale in India. Hence, the Multivariate Standardised Drought Index (MSDI) and Reconnaissance Trivariate Drought Index (RTDI) have been constructed that could be helpful in monitoring the drought in a detailed manner. For better understanding of the interaction process, the influence of anomalous large-scale circulations to MSDI and RTDI drought indices was evaluated. The MSDI and RTDI can provide the details regarding the onset and withdrawal information of drought to water managers for better monitoring of water resources.

2 Study area

The study area is the Godavari River basin, which covers an area of 3,12,810 km². Originating at an elevation of 1067 m near Triambakeswar in Nashik district, it flows over a total distance of 1465 km before emptying into the Bay of Bengal near Rajahmundry. The river basin lies between longitudes 73°24'E to 83°4'E and latitudes of 16°19'N to 22°34'N. The basin receives an average annual rainfall of about 1100 mm,

out of which more than 80% of the total rainfall occurs during south-west monsoon season. The annual precipitation varies from about 600 mm to about 1200 mm over the basin. The basin has a tropical climate and the average temperature varies between 15 °C in winter season and 45 °C in the peak of summer. The rainfall during the months of January and February is less than 15 mm which makes the river almost dry during this period. About 30% of the basin lies in water-deficit region. The maximum rainfall of the river basin occurs during the period from June to September. The entire river basin is undulating because of series of ridges that are formed in the low hill range. The basin geology consists of tertiary Deccan Traps, Archean Granites, Precambrian and Gondwana sedimentary rocks and recent alluvial cover. Black soils, lateritic soils, red soils, alluvium, mixed soils and saline and alkaline soils are predominant in the basin. Figure 1 shows the location map of study area.

2.1 Description of reference data

The assessment of drought indices requires a large amount of sufficiently long historic observations to obtain a reliable evaluation of drought phenomenon. This study used $0.5^\circ \times 0.5^\circ$ monthly gridded precipitation and

evapotranspiration data sets acquired for a period of 38 years (1980–2017) from Climate Research Unit Time series (CRU TS 4.03, https://data.ceda.ac.uk/badc/cru/data/cru_ts/cru_ts_4.03). The evapotranspiration data for the same time span was downloaded and extracted to a particular location for further analysis of RDI. CRU data was utilised for the temperature-based derivation of potential evapotranspiration (Harris et al. 2014). Gridded rainfall, evapotranspiration and temperature data have been extensively used in various hydro-climatological analyses in different parts of the world (Zarch et al. 2015; Krishnan et al. 2019). The VIC soil moisture data has been used in many studies and proved to be a reliable source to assess the soil moisture drought anomalies (Wang et al. 2011; Mishra et al. 2014). So, the soil moisture data for the period from 1980 to 2017 was downloaded from the GLDAS VIC data sets for further computation of SSI. For uniformity in the data, the soil moisture was regridded to CRU grids.

As discussed, CWA is performed between large-scale climate oscillations (SOI, SST, MEI, IOD and ISMR) and the developed drought indices. This helps to identify the teleconnections of climate indices with the drought indices. The large-scale climate indices used in this study are downloaded from links given in Table 1.

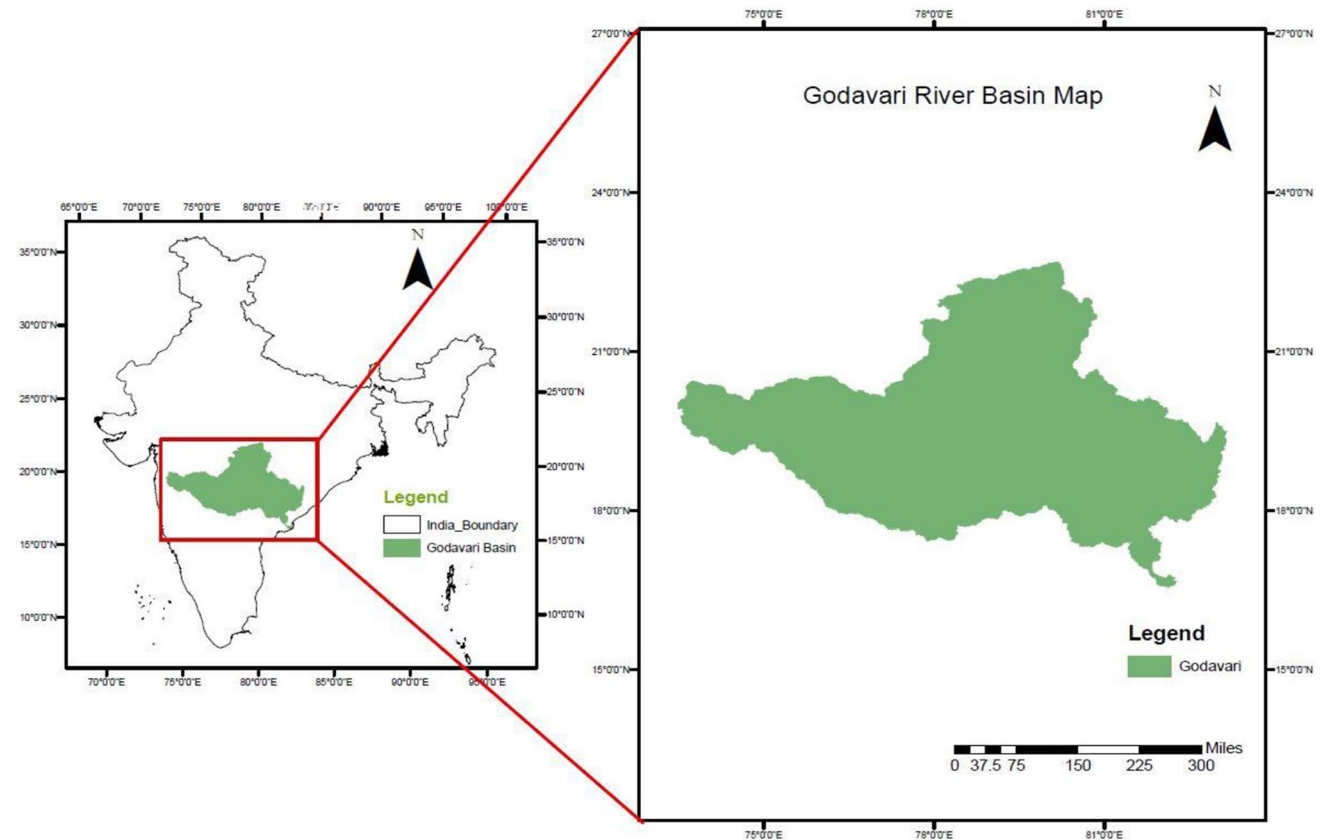


Fig. 1 Study area map of Godavari River basin

Table 1 Large-scale climate indices and their downloading links

Large-scale climate indices	Downloading links
SOI	http://www.bom.gov.au/climate/current/soihtml1.shtml
SST	http://www.esrl.noaa.gov/psd/gcos_wgsp/Timeseries/Data/nino34.long.anom.data
MEI	http://www.esrl.noaa.gov/psd/enso/mei.ext/table.ext.html
IOD	http://www.jamstec.go.jp/frcgc/research/d1/iod/DATA/dmi.monthly.txt
ISMIR	http://apdrc.soest.hawaii.edu/projects/monsoon/daily-data.html#montar

3 Methodology

3.1 Computation of SPI, RDI and SSI

SPI, RDI and SSI for 3- and 6-month time scales were computed for the Godavari River basin. SPI follows the two-parameter (scale and shape parameter) Gamma probability density function. Gamma (Γ) probability distribution used to describe precipitation variation is shown in Eq. 1.

$$G(x_n) = \frac{1}{\beta^\alpha \Gamma(\alpha)} x_n^{\alpha-1} \exp^{-x_n/\beta} \quad (1)$$

Gamma probability density function is applied to 3-month and 6-month moving average precipitation series in order to estimate SPI by involving a shape factor and a scale factor, termed as α and β respectively. The wet periods are specified by positive SPI series, whereas a sequence of negative values denotes a dry period.

RDI was proposed by Tsakiris et al. (2007) in which it was conceptualised that the meteorological droughts show the water balance deficit between precipitation and output reference evapotranspiration. The initial value (a_k) is a combined form using a monthly time-step and can be computed in terms of 3-month and 6-month time scales. RDI is calculated using Eq. 2.

$$a_k^{(i)} = \frac{\sum_{j=1}^k P_{ij}}{\sum_{j=1}^k \text{PET}_{ij}} \quad I = 1 \text{ to } \dots n \quad (2)$$

where P_{ij} and PET_{ij} are the precipitation and PET respectively of the j th month of the i th year.

It is assumed that the standardised RDI follows Lognormal distribution as given in Eq. 3

$$\text{RDI}_{\text{st}}(k)(i) = \frac{y_k^{(i)} - \bar{y}_k}{\sigma_{y_k}} \quad (3)$$

where y_k is $\ln(a_k)$, \bar{y}_k is the arithmetic mean of y and σ_{y_k} is its standard deviation. The calculation of RDI_{st} for monthly time steps, which may contain zero-precipitation values, can be carried out by the lognormal approach.

Alternatively, SSI can be computed by using empirical probability function instead of a parametric Gamma function. Farahmand and AghaKouchak (2015) derived the marginal probability of soil moisture from the GLDAS data site using the empirical Gringorten plotting position as given in Eq. 4.

$$P(X_n) = K = \frac{r - 0.44}{n + 0.12} \quad (4)$$

where ' n ' denotes the total sample size and r denotes the rank of soil moisture data which have non-zero values and $P(X_n)$ is the empirical probability. The outputs of Eq. (1) and Eq. (3) can be transformed into the Standardised Index (SI) as shown in Eq. 5.

$$\text{SI} = \Phi^{-1}(K) \quad (5)$$

where Φ is the standard normal distribution function and K is probability derived from Eq. 5. The computed SPI, SSI and RDI indices were further compared with the multivariate drought indices computed in this study.

3.2 Multivariate drought indices

3.2.1 Step 1: Copula analysis

Copula is rapidly gaining popularity as a modelling tool for multivariate data analysis. Copulas are used for analysing the flood and drought return period as well as an extensive range of problems in finance and managing the risk (Cherubini et al. 2004; Salvadori et al. 2013; Ganguli and Reddy, 2013; Daneshkhah et al. 2016; Das et al. 2020a, b). In this study, two copula families, namely Elliptical (Student's t and Normal) and Archimedean (Clayton, Gumbel and Frank) copula families are used.

The presence of a unique copula is assumed, but the most important aspect to be noticed here is the selection of a suitable copula function (Nelsen, 2006). The multivariate random vectors are denoted as $X = (X_1, \dots, X_d)$ with margins of F_x being continuous and strictly increasing. $F(X_1, \dots, X_d)$ is the joint probability distributions with margins as F_{x_1}, \dots, F_{x_d} . Then there must be a presence of

unique copula C for all $X_1, \dots, X_d \in [-\infty, \infty]$ which links the multivariate distribution and d dimensional copulas as provided by Eq. 6.

$$C_\theta(\alpha_1, \dots, \alpha_d) = Pr(F_{X_1}(X_1) \leq \alpha_1, \dots, F_{X_d}(X_d) \leq \alpha_d) = F_x(F_{X_1}^{-1}(\alpha_1), \dots, F_{X_d}^{-1}(\alpha_d)) \tag{6}$$

The values of X_1, \dots, X_d are the inverse functions of $\alpha_1, \dots, \alpha_d$

So, $X_1 = F_{X_1}^{-1}(\alpha_1), \dots, X_d = F_{X_d}^{-1}(\alpha_d)$

$$F(X_1, \dots, X_d) = C(F_1(X_1), \dots, F_d(X_d)) = Q \tag{7}$$

For bivariate case,

$$F(X_1, X_2) = C(F_1(X_1), F_2(X_2)) = Q \tag{8}$$

For trivariate case,

$$F(X_1, X_2, X_3) = C(F_1(X_1), F_2(X_2), F_3(X_3)) = K \tag{9}$$

The various types of copula used in this study are given by the relations given in Eq. 10 to Eq. 14:

Clayton:

$$C_\theta(\alpha, \beta) = (\alpha^{-\theta} + \beta^{-\theta} - 1)^{-\theta} \text{ for all } \theta \in (0, \infty) \tag{10}$$

Frank:

$$C_\theta(\alpha, \beta) = -\frac{1}{\theta} \log \left(1 + \frac{(\exp(-\theta\alpha) - 1)(\exp(-\theta\beta) - 1)}{\exp(-\theta) - 1} \right) \text{ for } \theta \in R \setminus \{0\} \tag{11}$$

Gaussian:

$$C_\theta(\alpha, \beta) = \int_{-\infty}^{\varphi^{-1}(\alpha)} \int_{-\infty}^{\varphi^{-1}(\beta)} \frac{1}{2\pi\sqrt{1-\theta^2}} e^{\frac{2\theta uv - u^2 - v^2}{2(1-\theta^2)}} dudv \tag{12}$$

Gumbel:

$$C_\theta(\alpha, \beta) = \exp\{-[-(-\log\alpha)^\theta + (-\log\beta)^\theta]^{1/\theta}\}, \text{ for } \theta \in [1, \infty) \tag{13}$$

Student's t :

$$C_\theta(\alpha, \beta) = \int_{-\infty}^{T_r^{-1}(\alpha)} \int_{-\infty}^{T_r^{-1}(\beta)} \frac{\Gamma\left(\frac{\nu+2}{2}\right)}{\Gamma\left(\frac{\nu}{2}\right)\nu\pi\sqrt{1-\theta^2}} \left\{1 + \frac{u^2 + v^2 - 2\theta uv}{\nu(1-\theta^2)}\right\} dudv \tag{14}$$

3.2.2 Step 2: Measure of dependence of copulas

While modelling by the multivariate approach, there must be an involvement of a significant non-linear degree of dependence between the variables. To deal with the linear

dependency structure, Kendall's τ and Spearman's ρ rank correlation methods were used.

3.2.3 Step 3: Parameter estimation

The maximum-likelihood method typically comprises of estimating the parameters of copula-based joint distribution. Depending on the marginal distribution, the optimised parameter of the copula family is numerically achievable through joint probability density function. Each parametric marginal is associated with the copula likelihood, which is maximised on the basis of copula parameters. Since the marginals are treated as nuisance parameters, the best way is to proceed with the pseudo-samples $(\alpha_1, \dots, \alpha_n)$, which is demonstrated as a non-parametric method of estimation. The parameter estimation of copula function is greatly advanced by the pseudo-maximum-likelihood estimator (Kim et al. 2007; Nguyen and Jayakumar, 2018).

3.2.4 Step 4: Goodness of fit

The concept of copula allows for the estimation of marginal distributions and the joint probability density function separately, but the main intention to fit multivariate distribution is frequently ignored. Here, the pseudo-samples are used for the non-parametric method of estimation of parameters for copulas. The most natural choice for goodness of fit (GoF) tests are Cramer-von Mises (T_{cvm}), chi-square (Ch_{sq}) and Kolmogorov-Smirnov (S_{ks}) tests as well as Akaike Information Criteria (AIC), which are the procedures frequently used in hydrology. These criteria can be applied for obtaining the best fitted copula by comparing the p -values obtained from all the GoF tests (Genest et al. 2009).

3.2.5 Step 5: MSDI and RTDI calculation

The MSDI can be computed using the joint probability Q as given in Eq. 15.

$$MSDI = \varphi^{-1}(Q) \tag{15}$$

For the computation of RTDI, the joint probability given in Eq. (9) can be used. The link between the joint probability of K and the RTDI can be derived using Eq. 16

$$RTDI = \varphi^{-1}(K) \tag{16}$$

where φ^{-1} is the inverse standard normal distribution function. MSDI is formulated as the joint probability of precipitation and soil moisture. RTDI defines the integration of precipitation, soil moisture and evapotranspiration. The SPI and SSI have been taken for cross comparison with

MSDI. Similarly, a comparison of RDI and SSI with RTDI was carried out to identify the variations in multivariate drought conditions. Similar to SPI, the MSDI and RTDI can also have negative values, which imply the dry period. Positive values imply the wet period and the zero values of the drought refer to normal climate conditions.

3.3 Modified Mann–Kendall (MMK) test

A non-parametric Modified Mann–Kendall (MMK) trend test approach is applied in this study for the Godavari River basin to observe the respective trend in the time series of n -month (3 and 6 months) MSDI and RTDI (Hamed and Rao, 1998). The MMK method takes into account the lag- i autocorrelation to eliminate the persistence (Huang et al. 2015). In this study, the normalised test statistic (Z) with 95% confidence level was used for a qualitative assessment of the trend associated with the multivariate drought signals. The description of the framework of estimation of MSDI and RTDI is presented in Fig. 2.

3.4 Cross-wavelet analysis

The combination of cross-wavelet transform (XWT) and the cross-wavelet spectrum (CWS) can be represented by CWA. CWA breaks down the time series into time and frequency domain and detects the significant association with other variable (Tan et al., 2016; Vazifekhhah and Kahya, 2019; Himayoun and Roshni, 2019). This method identifies the combined teleconnection and the variations in the time and frequency domain of the pair time-series. Morlet wavelet is adopted as mother wavelet as it shows a good balance between time and frequency localization. Therefore, the CWA is implemented to examine the potential teleconnection between SOI/IOD/SST/MEI/ISMR events with both MSDI and RTDI time series. The two-time series are taken as α_k and β_k and the XWT for these time series is shown in Eq. 17.

$$W^{\alpha\beta} = W^\alpha W^{\beta*} \quad (17)$$

where $*$ denotes the complex conjugate and the cross-wavelet power (CWP) is denoted as $|W^{\alpha\beta}|$. The distribution associated with the CWP of α_k and β_k with the related power spectra P_n^α and P_n^β is given in Eq. (18)

$$D\left(\frac{|W_n^\alpha(s)W_n^{\beta*}(s)|}{\sigma_\alpha\sigma_\beta} < p\right) = \frac{Z_{v,(p)}\sqrt{P_n^\alpha P_n^\beta}}{v} \quad (18)$$

where $Z_{v,(p)}$ is denoted as 95% the confidence level linked with the probability p . For more details regarding the CWA, the study by Grinsted et al. (2004) can be referred.

4 Result and discussions

4.1 SPI, RDI and SSI calculation

SPI, RDI and SSI were computed by using the method discussed previously. The values of these indices lying between 0 and -0.99 , -1.00 and -1.49 , -1.50 and -1.8 , and greater than -1.8 , define mild, moderate, severe and extreme drought. The negative drought index values were considered for estimation of dry events and the positive drought values were considered for wet periods. Run theory analysis proposed by Yevjevich (1967) is carried out in this study to characterise the drought events such as drought peak, duration and severity. A run is represented as part of the time series where all the entries are below the threshold value (Dixit et al. 2021). In this study, the threshold level is taken as -1 for estimating drought variables.

4.2 Bivariate dependency measurement

The dependency between precipitation and evapotranspiration, precipitation and soil moisture and evapotranspiration-soil moisture has been carried out using rank-based dependency measurement techniques like Kendall's τ and Spearman's ρ rank correlation coefficients were used. The analysis from Table 2 showed that best correlation is observed between precipitation and soil moisture whereas negative correlation exists between both precipitation-evapotranspiration and evapotranspiration-soil moisture. However, it may be argued that the dependence pairs (precipitation-evapotranspiration and evapotranspiration-soil moisture) are not significantly positive and that does not indicate that it is independent because other than normality condition, the zero correlation is similar to the dependency of parameters (Genest et al. 2007). Moreover, from a hydrological point of view, precipitation, evapotranspiration and soil moisture are dependent upon each other. Then the MSDI and RTDI were developed based on the parameters obtained for the best fitted copula.

4.3 Copula-based joint probability bivariate and trivariate analyses

The bivariate model is derived using the joint probability distribution of the precipitation and soil moisture. The information on precipitation and soil moisture is combined using Frank, Gumbel and Clayton copulas. Furthermore, a trivariate analysis has been carried out using the joint probability distribution of precipitation, soil moisture and evapotranspiration using meta-elliptical copulas (Student's t copula and Normal copula) as the process of evapotranspiration

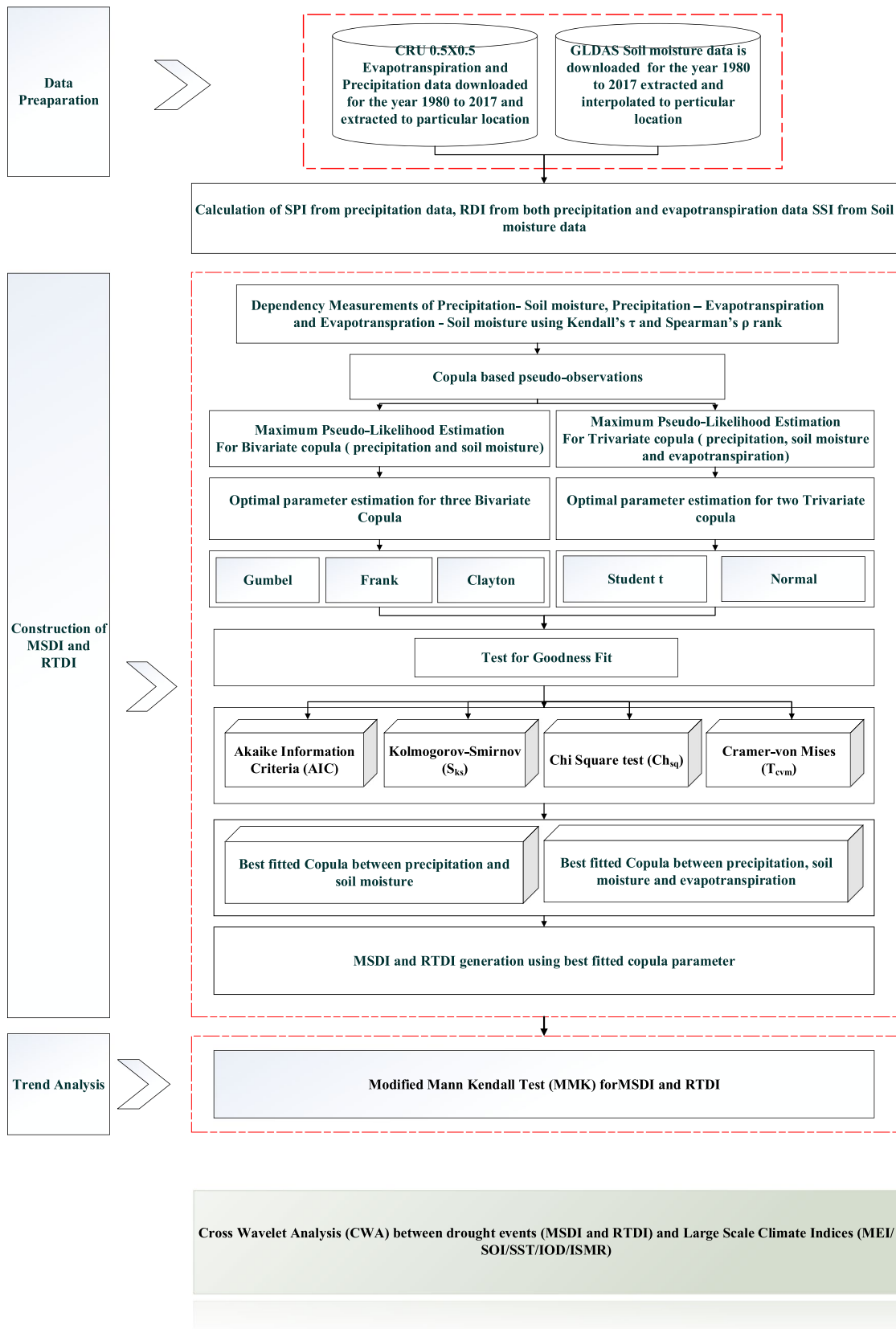


Fig. 2 Framework of estimation of bivariate drought and trivariate drought

Table 2 Dependency measurements of precipitation-soil moisture, evapotranspiration-precipitation and evapotranspiration and soil moisture

Variable	Kendall's τ	Spearman's ρ
1. Precipitation and soil moisture	0.307	0.477
2. Evapotranspiration and precipitation	-0.123	-0.164
3. Evapotranspiration and soil moisture	-0.34	-0.517

cannot be neglected from climatological point of view. The parameters of copulas were estimated using a rank-based pseudo-likelihood estimation (MPL). The GoF tests — S_{ks} , T_{cvm} , Ch_{sq} (for 1000 sample runs) and AIC justified the best copula for both bivariate and trivariate formulations of drought indices. The estimated parameters for copulas and their respective values are given in Table 3 and Table 4. The dependence between precipitation and soil moisture can be modelled by Frank copula since the GoF measures showed higher values and AIC showed lower values (Table 3). This can further be used for the computation of MSDI based on the parameters obtained from Frank copula. Table 4 describes that the trivariate analysis modelled by Student's t copula. Though the p -value greater than 0.05 cannot be ignored in the copula formation, but in this case, the best fitted copulas (Frank and Student's t copula) are chosen for further analysis of MSDI and RTDI.

4.4 Comparison between SPI, SSI and MSDI

SPI shows the behaviour of meteorological drought which has a faster onset and offset of drought behaviour. SSI is for the agricultural drought which depends on the temperature, soil characteristics and soil groups dominant in the particular area. The combination mechanisms of SPI, SSI and MSDI can be understood in a better way by dividing the whole time series into two parts, viz. 1981–1999 and 2000–2017. However, perfect correlations may not exist between SPI, SSI and MSDI but they may follow the same drought evolution pattern. Figure 3a shows that some there are some signals which showed agreements and some which showed disagreements between SPI, SSI and MSDI. SSI-3 showed a moderate drought condition in April 1987 while MSDI showed an extreme drought condition for the same time period.

Table 3 p -values for the GoF tests — S_{ks} , T_{cvm} and Ch_{sq} for deriving 3 months and 6 months based on Gumbel, Frank and Clayton copulas using precipitation and soil moisture.

3 months	Gumbel	Frank	Clayton	6 months	Gumbel	Frank	Clayton
S_{ks}	0.7	0.81	0.4	S_{ks}	0.66	0.74	0.41
Ch_{sq}	0.1	0.21	0.3	Ch_{sq}	0.19	0.46	0.3
T_{cvm}	0.5	0.9	0.2	T_{cvm}	0.36	0.27	0.29
AIC	-105.9	-117.9	-32.7	AIC	-135.87	-143.1	-63.96
θ^{PML}	1.4	3.2	0.4	θ^{PML}	1.5	3.69	0.58

Table 4 p -values for the GoF tests — S_{ks} , T_{cvm} and Ch_{sq} for deriving 3 months and 6 months based on Student's t copula and Normal copula using precipitation, soil moisture and evapotranspiration.

3 months	Student's t	Normal	6 months	Student's t	Normal
S_{ks}	0.35	0.02	S_{ks}	0.26	0.25
Ch_{sq}	0.4	0.39	Ch_{sq}	0.41	0.4
T_{cvm}	0.46	0.31	T_{cvm}	0.28	0.11
AIC	-272.8	-149.16	AIC	-277.31	-189.52
θ^{PML}	0.55	0.54	θ^{PML}	0.54	0.54

October-1986 showed a severity in drought behaviour with respect to SPI-3, SSI-3 and MSDI-3. More fluctuations in drought signals occurred in the 3-month MSDI time series. It can be clearly observed that the 3-month MSDI and SSI drought condition continued from September 1996 to May 1998 (Fig. 3a). For the period from 2001 to 2010, the SPI-3 showed recovery from drought when compared to SSI-3 and MSDI-3. The time period (2000–2017) showed negative values that indicated that the drought continued from the year 2011 to 2013, whereas positive drought continued between September 2013 and September 2014. Severe drought conditions are observed again in the year June 2015–2016. It is seen that the MSDI showed combined effect of SPI and SSI.

In the time window of 1981–1999, SSI-6 showed early recovery of drought when compared to SPI-6 while the MSDI-6 showed higher negative drought trend when compared to SSI and SPI. Drought severity is observed during May 1985 as both the precipitation and soil moisture have negative trend and as a result of this, the MSDI-6 showed a severe drought condition (a combination of SPI and SSI). The SPI-6 showed moderate drought condition whereas MSDI-6 showed severe drought conditions during the period January 1992 to May 1992 and May 1997 to September 1997. SPI-6 showed that most of the drought signals are having positively trending values whereas SSI-6 showed most of the signals have negative drought conditions for the time period 2001–2010. MSDI-6 showed peak drought conditions from May to September 2001 and January to May 2005. The severity of drought can clearly be noticed during May 2012, April to May 2013 and December 2015 for MSDI-6 whereas SPI-6 showed moderate drought conditions. It is, hence, evident that when

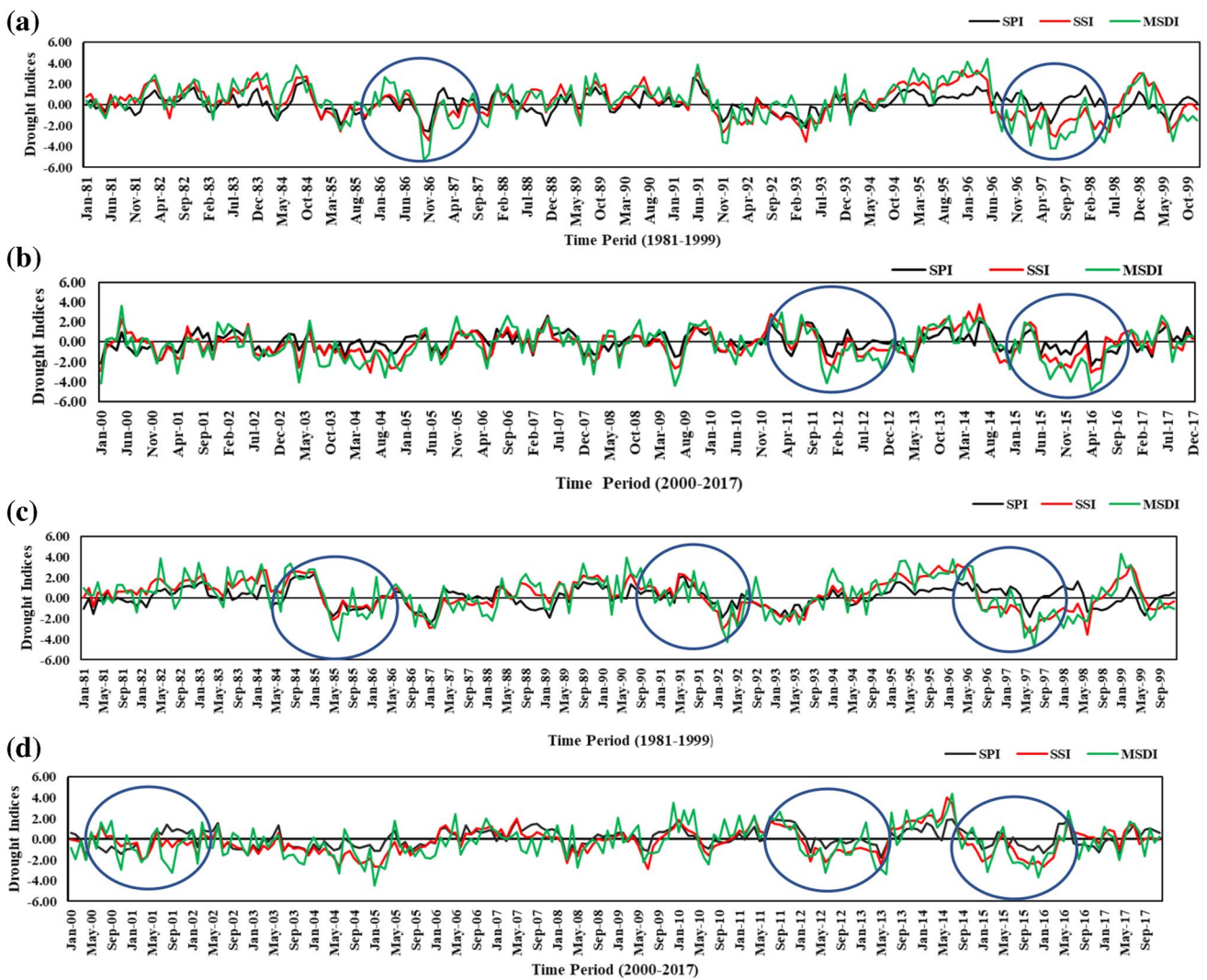


Fig. 3 Comparisons of SPI, SSI and MSDI for 3-month and 6-month time scale; **a** 3-month time scales during the time window 1981–1999; **b** 3-month time scales during the time window 2000–2017; **c**

6-month time scales during the time window 1981–1999; **d** 6-month time scales during the time window 2000–2017

the drought duration increased from 3 to 6 months, less difference in drought trend is observed between SPI and SSI whereas the MSDI showed more fluctuating drought conditions.

4.5 Comparison of RDI, SSI and RTDI

The RTDI is compared with RDI and SSI. RDI is chosen because it gives combined drought information of precipitation and evapotranspiration. Precipitation alone cannot be used for the detection of drought. The RDI-3 and SSI-3 are generally consistent but discontinuity is also observed between time signals. It can be observed from Fig. 4a that the time signals show that the positive and negative drought signals are different. For example, May 1998 showed a

positive trend in RDI-3 and a negative trend for SSI-3. Ultimately, a negative RTDI-3 emerged in this case. If the average rainfall is more and evapotranspiration is less ($RDI > 0$) and the soil moisture is dry ($SSI < 0$) for that period of time, then the combination of the three variables (RTDI) can create a negative drought trend ($RTDI < 0$). For a 3-month time scale, the drought duration of RTDI signals is similar to SSI. The severity aspect of drought must not be neglected in this circumstance. During the years 1981 to 1999, it can be observed that SSI showed more negative drought trends than RDI. So RTDI showed a drought event whichever is lower between RDI and SSI. The peak drought is seen in May 1984, April 1985 and September 2016 for RTDI-3. However, the extremely dry months for RDI are May 1985, December 2000, January 2001 and May 2014 and for SSI June 1980,

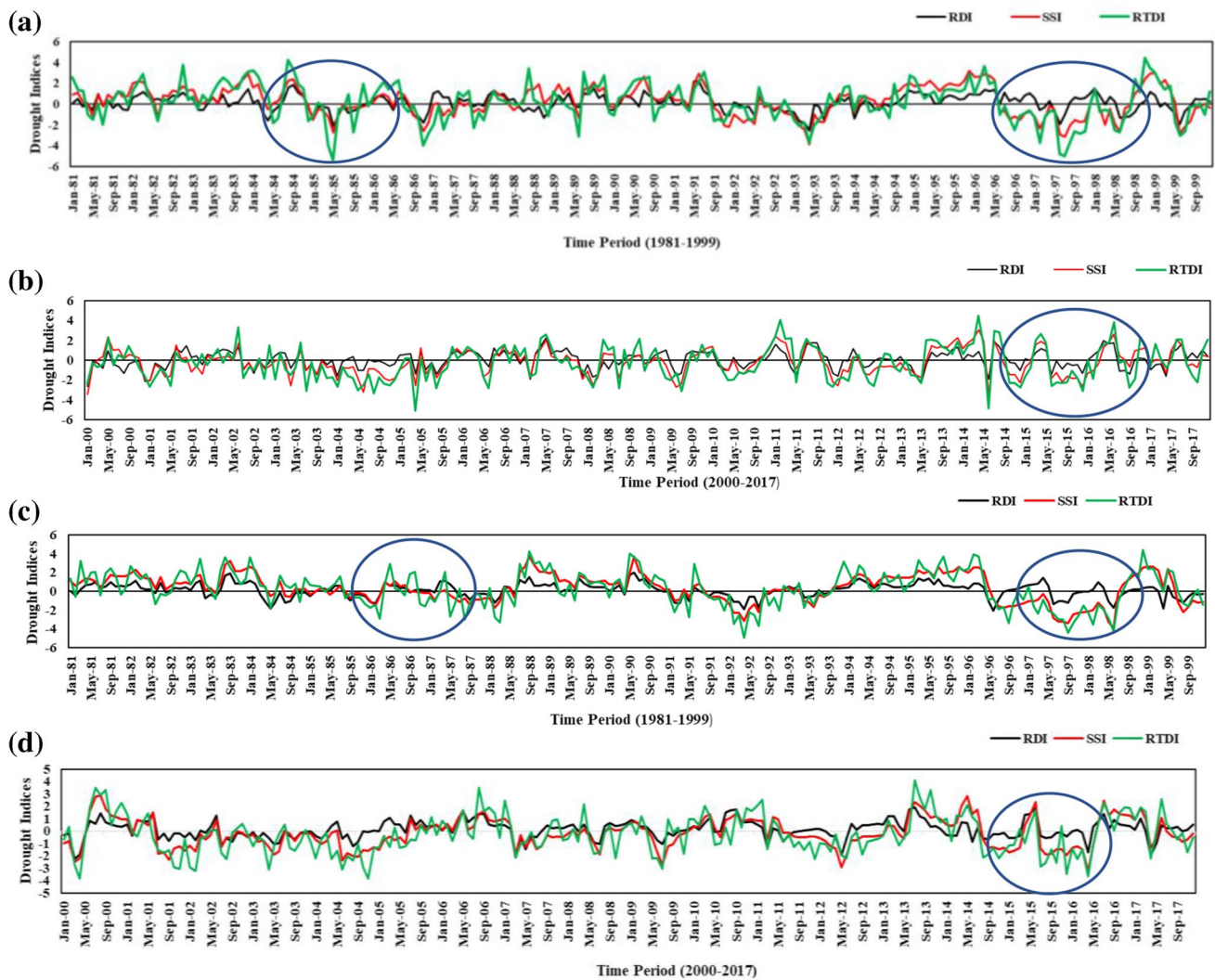


Fig. 4 Comparisons of RDI, SSI and RTDI for 3-month and 6-month time scale. **a** 3-month time scales during the time window 1981–1991; **b** 3-month time scales during the time window 2000–2017; **c**

6-month time scales during the time window 1981–1991; **d** 6-month time scales during the time window 2000–2017

March 1987, August to November 1997, January to May 1998 and May 2006.

The initial drought is captured by RTDI-6 as shown in Fig. 4c. The drought peaks are more prominent in RTDI-6 as compared to RDI-6 and SSI-6. In January 1986, it is observed that negative signals of drought are captured for both RDI-6 and SSI-6. So the RTDI-6 also followed these negative trends of the drought indices. For the year 2016, negative drought effect of RTDI is observed due to the combined effects of the RDI and SSI. RTDI captured drought earlier than SSI and RDI. In most of the cases, the drought condition is captured well for RTDI and SSI whereas RDI is not that so efficient in capturing the dry

events in the chosen 38 years of time frame. The drought duration and severity of the drought were different for RDI-6, SSI-6 and RTDI-6. The drought was more severe in the case of RTDI-6.

4.6 Comparison between MSDI and RTDI

MSDI and RTDI have been estimated using copula functions for 3- and 6-month time scales during the period 1981–2017. Here the hypothesis contains a comparison between MSDI and RTDI for better understanding of droughts based on different climatic parameters. Similar evolution pattern between MSDI and RTDI is observed during the period 1981–1999

(Fig. 5a). After analysing the data, it can be observed that there is an agreement and disagreement of drought signals between the MSDI and RTDI. The soil moisture anomaly status can influence the drought persistence and continuity between MSDI and RTDI. For example, an agreement between signals is visible in the time period of 1991–1992 and disagreements of time signals are visible in the time period of 1984–1985. The onset and offset of drought events for MSDI and RTDI are different. So there is a probability that the drought characteristics (severity and duration) must be different for these two indices. For example, RTDI-3 conveyed a severe drought condition in September 1985, whereas MSDI-3 showed a mild drought phenomenon. September 2004 and 2011 showed severe drought conditions for MSDI-3 and RTDI-3. So, the drought indices showed consistency with each other. It is evident that the 3-month drought signals displayed more variations when compared to 6-month drought signals. For example, January 1986 showed severity drought pattern for MSDI-6 and RTDI-6.

More consistency between signals is observed in the case of 6-month MSDI and RTDI (Fig. 5c and Fig. 5d).

MMK trend test, shown in Table 5, is used for the better evaluation of the temporal conditions of drought. For the selected location (East Godavari region), the result provided an identification of the trend associated with *n*-month MSDI and RTDI. MSDI-3 showed a significant negative trend whereas 3-month RTDI showed a positive trend in drought time series. However, for the 6-month time window, MSDI and RTDI drought signals showed significant negative trends.

Table 5 The trends of 3-month and 6-month MSDI and RTDI at 95% significance level

Time scales	Z statistic of MSDI	Z statistic of RTDI
3 months	-4.93	0.173
6 months	-0.3	-0.43

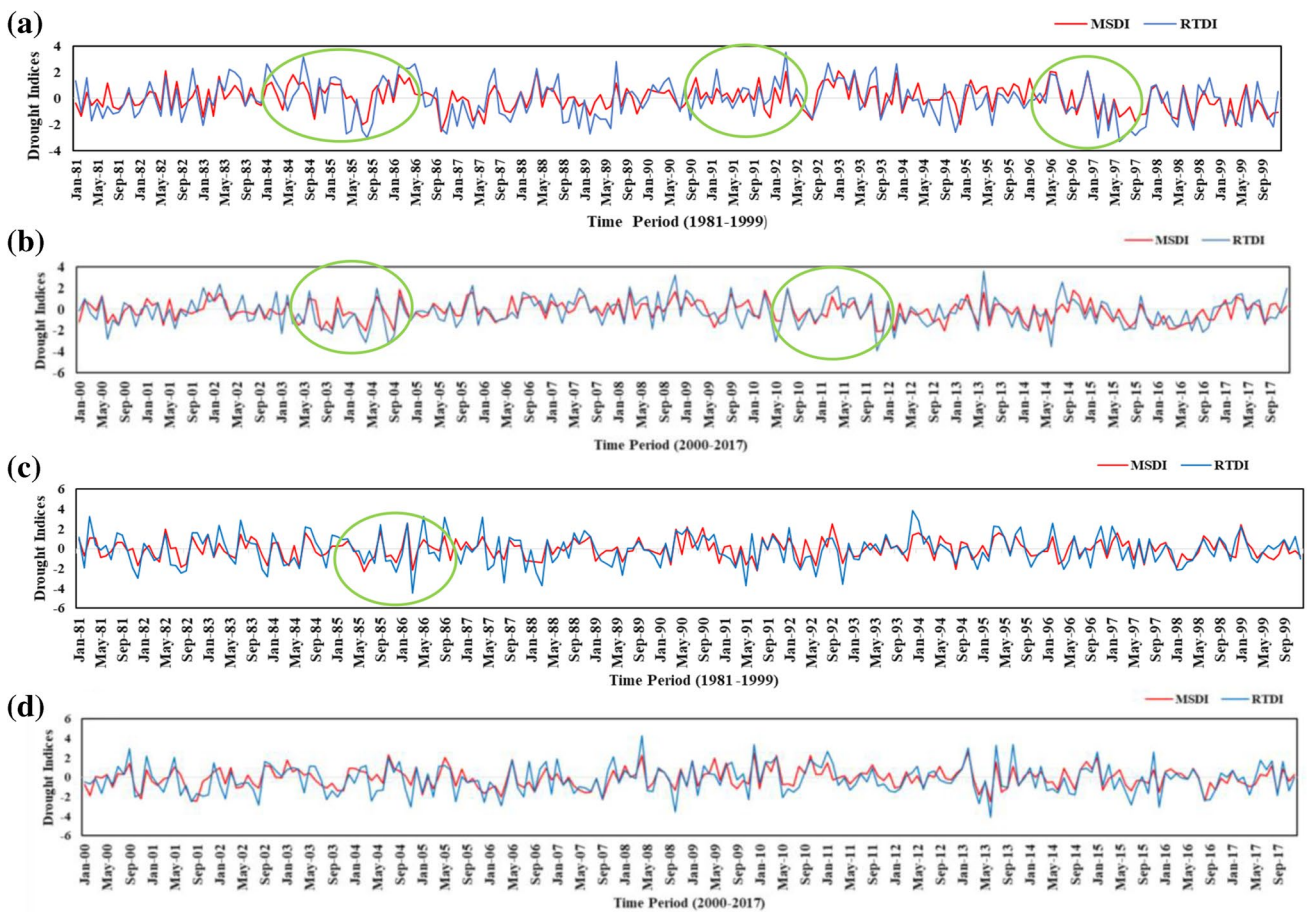


Fig. 5 Comparisons of MSDI and RTDI for 3-month and 6-month time scale. **a** 3-month time scales during the time window 1981–1999; **b** 3-month time scales during the time window 2000–2017; **c**

6-month time scales during the time window 1981–1999; **d** 6-month time scales during the time window 2000–2017

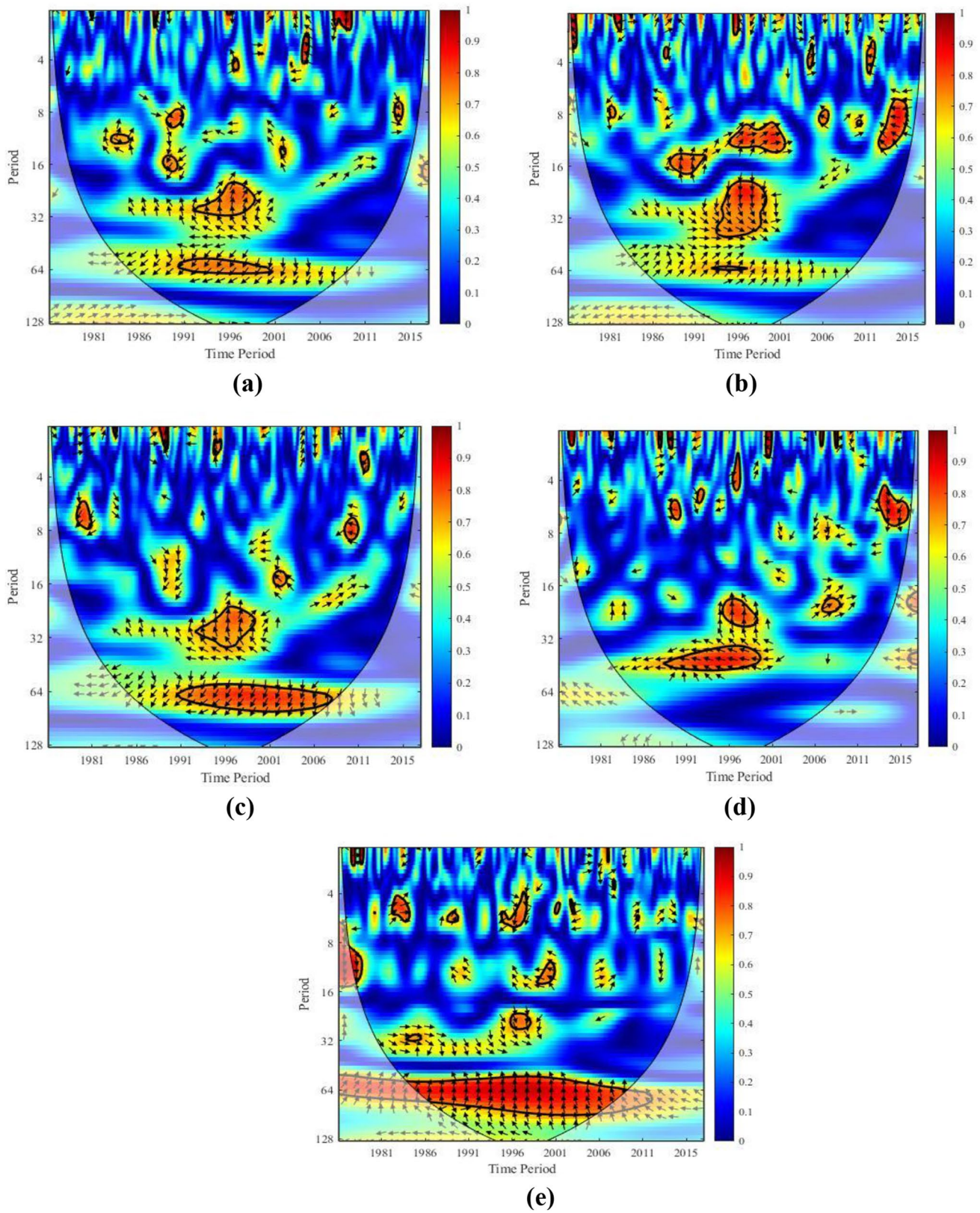


Fig. 6 The wavelet coherences between MSDI and large-scale climate indices for 3-month time scale. **a–c** The wavelet coherences between MSDI and MEI/SOI/SST; **d–e** the wavelet coherences between MSDI and IOD/ISMR

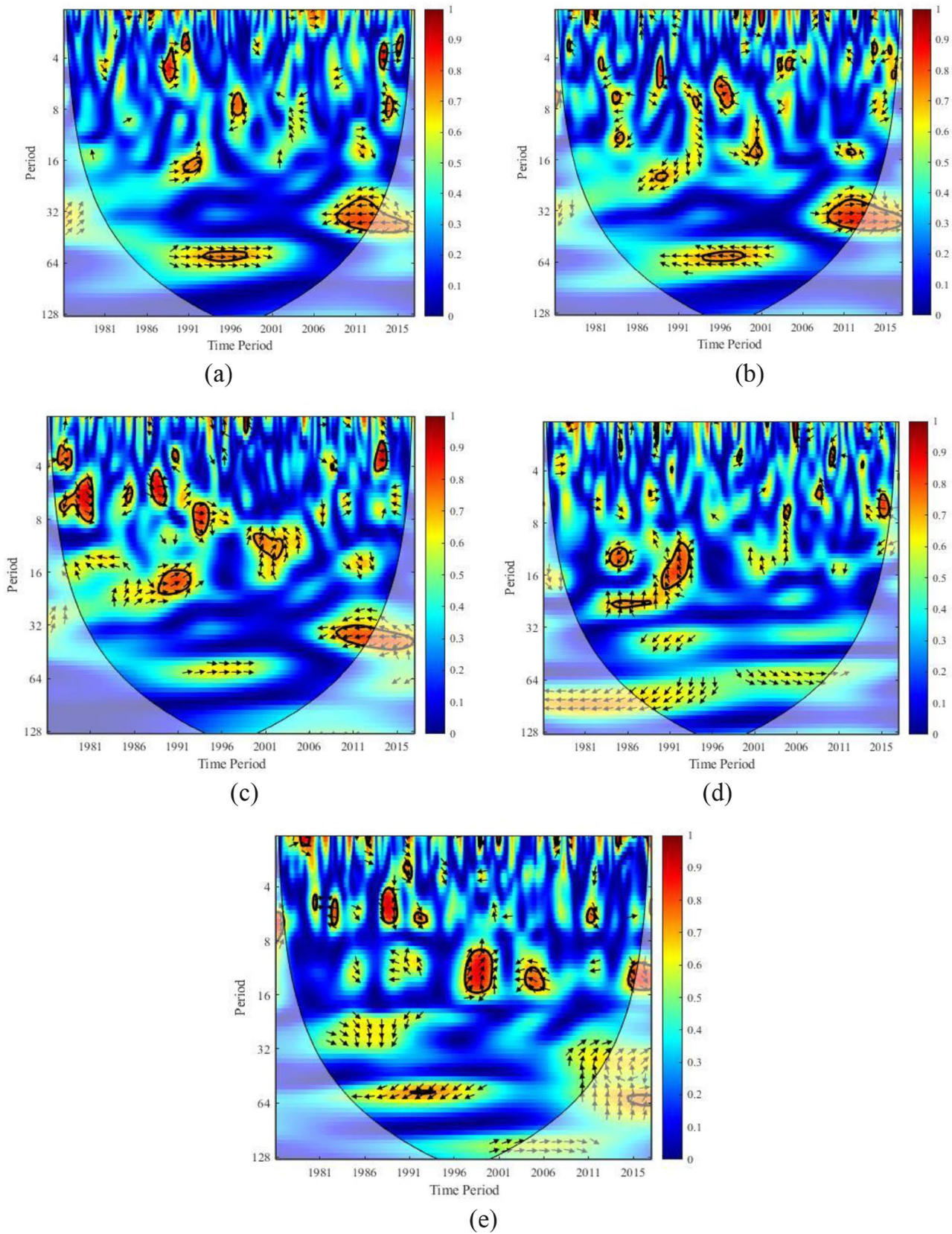


Fig. 7 The wavelet coherences between RTDI and large-scale climate indices for 3-month time scale. **a–c** The wavelet coherences between RTDI and MEI/SOI/SST; **d–e** the wavelet coherences between RTDI and IOD/ISMR

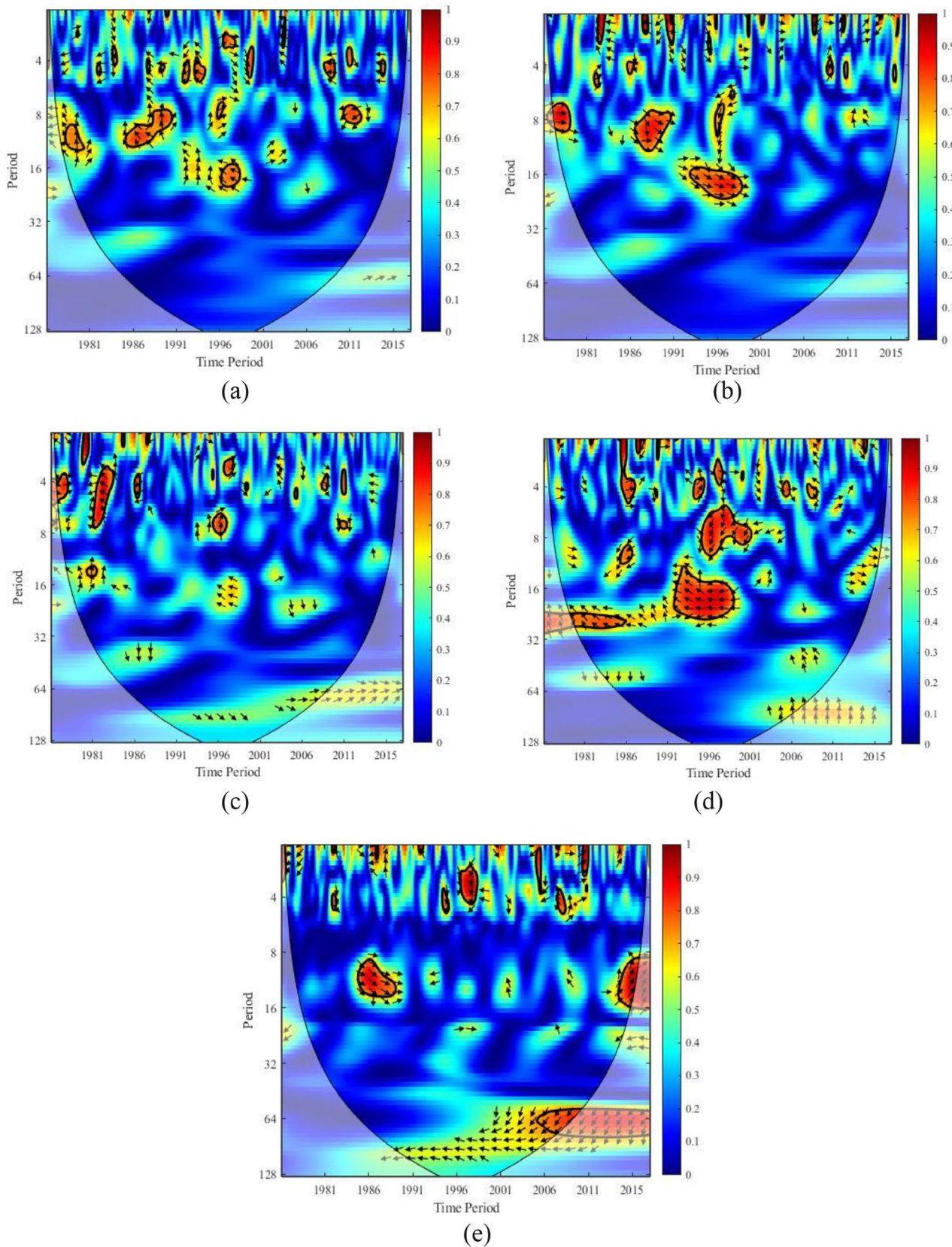


Fig. 8 The wavelet coherences between MSDI and large-scale climate indices for 6-month time scale. **a–c** The wavelet coherences between MSDI and MEI/SOI/SST; **d–e** the wavelet coherences between MSDI and IOD/ISMR

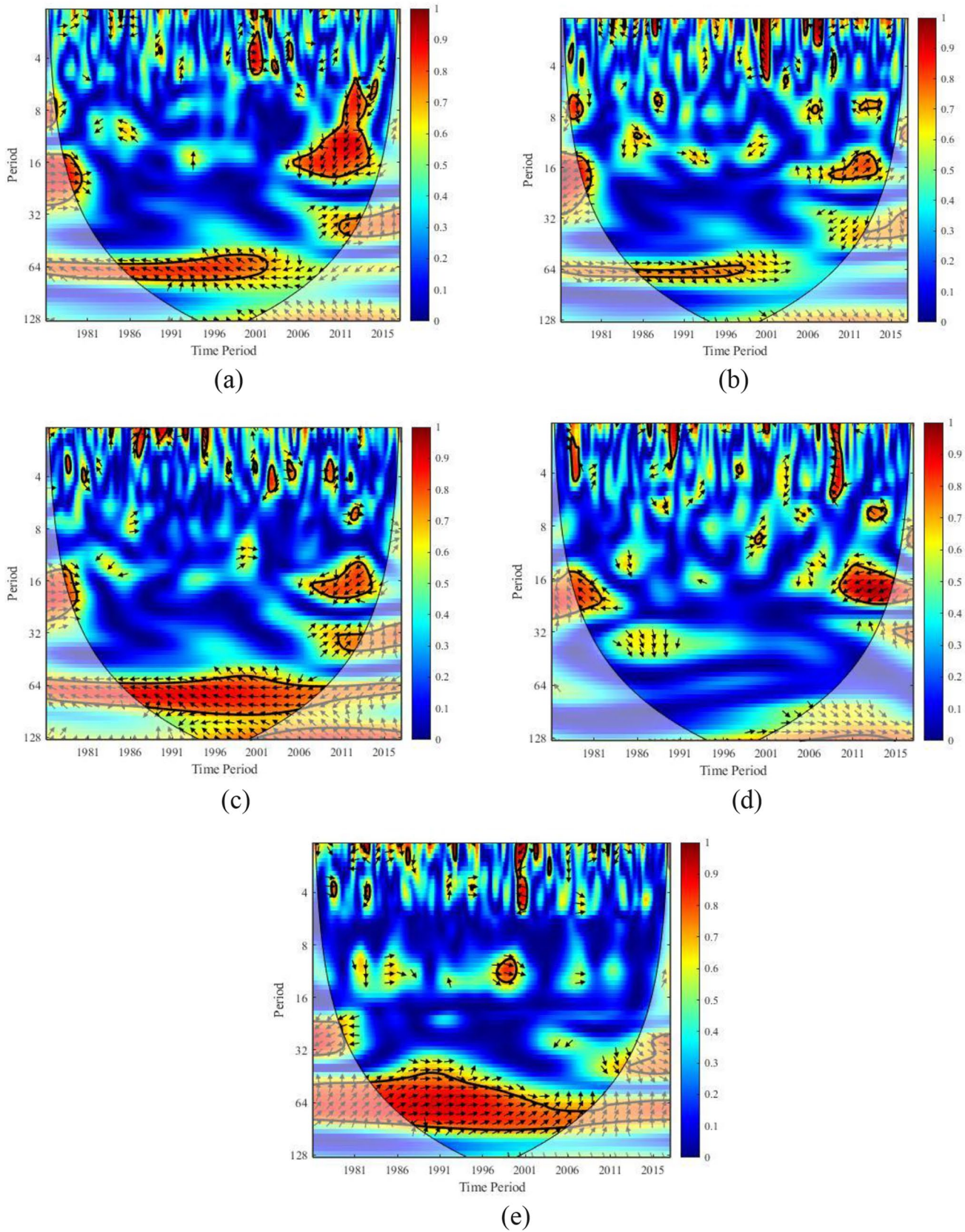


Fig. 9 The wavelet coherences between RTDI and large-scale climate indices for 6-month time scale. **a–c** The wavelet coherences between RTDI and MEI/SOI/SST; **d–e** the wavelet coherences between RTDI and IOD/ISMR

4.7 The teleconnection between MSDI and RTDI with large-scale climate indices

A number of studies have been carried out for variabilities of drought characteristics in India using CWA (Joshi et al., 2016; Kumar et al., 2021a). Kumar et al (2013) identified that the ENSO events have significant impact on the droughts occurring at the monsoon season over India. They also conveyed that the El Nino and La Nina showed different influence on drought variables over India. So, this study focussed on the effect of ENSO events, IOD and ISMR on MSDI and RTDI (3 and 6 months) for the Godavari basin. The teleconnection between the MSDI and RTDI climate indices with ENSO events, IOD and ISMR will be helpful for understanding the variability of meteorological and agricultural drought. Hence, CWA is implemented in this study for investigation of the association among drought indices and large-scale climate indices.

The wavelet coherences between monthly MSDI and RTDI with climate indices (MEI/SST/SOI/IOD/ISMR) in East Godavari region are illustrated in Fig. 6 and Fig. 7 respectively for 3-month time scale for the time period of 1981–2015. For 6-month time scale, MSDI and RTDI are represented in Fig. 8 and Fig. 9 respectively. The energy densities are represented by the colour bars. The arrows represent the phase relationship. The arrows pointing left show anti-phase relationship while the right pointed arrows define in-phase relationship and the 95% confidence level against red noise is given as a thick contour. Figure 6a displays a correlation pattern with MEI signals during 1991–1998 and 2013–2011. It can be observed from Fig. 6b that the SOI signals revealed a strong coherence pattern with MSDI-3 during 1988–1998 and 2012–2015 in the basin. Figure 6c displays a correlation of SST with drought signals (MSDI-3) during 1991–2007 whereas IOD exhibited a significant correlation with MSDI-3 during 1981–1985, 1988–1994 and 2011–2015 represented in Fig. 6d. Figure 6e displays that ISMR has a strong correlation with MSDI-3. ISMR displayed a strongest teleconnection pattern with MSDI-3 among all the large-scale climate indices.

The RTDI-3 showed teleconnections with MEI and SOI as given in Fig. 7a–b. In Fig. 7b, SOI showed a statically significant coherence with RTDI-3 during 1992–1997 and 2010–2015 at the 95% significance level. For RTDI-3, the teleconnections with SST are observed in Fig. 7c. The most evident teleconnection with SST and RTDI-3 is observed during the period 2006–2015 and SST confirmed a strongest correlation pattern with RTDI-3 as compared to other climate indices. IOD also demonstrated a strong teleconnection pattern with RTDI-3 during 1983–1990 and 2013–2015 illustrated in Fig. 7d. As given in Fig. 7e, the ISMR signals showed a fairly good association with RTDI-3 series. The coherence patterns of MSDI-6 and large-scale

climate indices are given in Fig. 8a to e. It can be seen that MEI exhibited a statistically significant teleconnection with MSDI-6 with during 1988–2010 at 95% significance level as seen in Fig. 8a. From Fig. 8c, the strongest correlation is identified between the MSDI-6 and SST signals. The SOI, IOD and ISMR revealed a fairly good correlation with MSDI-6 drought events in the East Godavari region. Figure 9a describes a good correlation of RTDI-6 with MEI during 1981–2001 and 2011–2015. RTDI-6 also exhibited a good teleconnection with SOI, SST, IOD and ISMR. From Fig. 9c to e, it can be confirmed that the RTDI-6 showed a significant and strong correlations with SST and ISMR. Hence, it can be concluded based on the observations from CWA that SST and ISMR emerged as the most significant indices which can impact the meteorological and agricultural droughts in this region. These are reflected in the variations of MSDI and RTDI, which have been developed in the study.

5 Conclusions

The integration of agricultural and meteorological drought plays a vital role in the prediction and reliable monitoring of drought. In this study, a copula-based MSDI and RTDI were developed for a clear representation of meteorological and agricultural features of drought in the hydrological process.

From the study, it is observed that MSDI and RTDI are important for capturing a quantitative and qualitative drought which consists of both agricultural and meteorological drought occurrences to examine the evolution of drought phenomenon.

These indices are applied to study the drought in the Godavari River basin, one of the largest river basins in India. Furthermore, copula analysis showed that the parameters of Frank copula can be used for obtaining the MSDI while Student's *t* copula can be used for obtaining RTDI.

The resultant MSDI and RTDI are based on the joint probability cumulative distribution function whose sensitivity towards capturing the persistence, onset and termination of drought is more prominent than SPI, RDI and SSI. This can help in understanding the real-time spatial as well as temporal drought mechanism. It also can help in early detection of drought condition rather than SPI, RDI and SSI.

The MMK test statistics considering the lag-*i* have given a strong indication of the trend associated with the time series of MSDI and RTDI. Overall, the trend analysis investigated showed that a negative trend is observed in MSDI and a positive trend is associated with RTDI.

CWA is performed in this study to identify the teleconnections between large-scale climate indices and the drought events. CWA showed MSDI and RTDI (3 and 6 months) have been significantly influenced by ENSO, IOD and ISMR patterns. Among all the climate indices, ISMR showed a

strong and effective association with MSDI-3 whereas SST revealed a strong teleconnection with RTDI-3. Additionally, SST has a strong influence on MSDI-6 and RTDI-6 showed a strong association with SST and ISMR signals. So, it can be suggested that the ENSO events, IOD and ISMR play a major role in drought variability over this basin.

MSDI and RTDI can capture the meteorological and agricultural drought variability detecting the onset and termination of droughts. These multivariate drought indices will be beneficial in deeper understanding of the drought mechanisms and further enhance the drought monitoring technology. Overall, the study showed the teleconnection of MSDI and RTDI with large-scale climate indices can be potentially used for drought monitoring and assessment under the climate variability in India.

Author contribution Soumyashree Dixit — conceptualization, data curation, formal analysis, investigation, methodology, resources, software, validation, visualization and writing — original draft; K V Jayakumar — project administration, supervision and writing — review and editing.

Data availability All data are available in the given website.

Code availability All codes are available from the corresponding author upon request.

Declarations

Ethics approval None

Consent to participate Informed consent was obtained from all individual participants included in the study.

Consent for publication The participants have consented to the submission of the research article to the journal.

Conflict of interest The authors declare no competing interests.

References

- Cherubini U, Luciano E, Vecchiato W (2004) Copula methods in finance. Wiley
- Daneshkhah A, Remesan R, Chatrabgoun O, Holman IP (2016) Probabilistic modeling of flood characterizations with parametric and minimum information pair-copula model. *J Hydrol* 540:469–487. <https://doi.org/10.1016/j.jhydrol.2016.06.044>
- Das J, Jha S, Goyal MK (2020a) Non-stationary and copula-based approach to assess the drought characteristics encompassing climate indices over the Himalayan states in India. *J Hydrol* 580:124356. <https://doi.org/10.1016/j.jhydrol.2019.124356>
- Das J, Jha S, Goyal MK (2020b) On the relationship of climatic and monsoon teleconnections with monthly precipitation over meteorologically homogenous regions in India: wavelet & global coherence approaches. *Atmos Res* 238:104889. <https://doi.org/10.1016/j.atmosres.2020.104889>
- Dixit S, Tayyaba S, Jayakumar KV (2021) Spatio-temporal variation and future risk assessment of projected drought events in the Godavari River basin using regional climate models. *J Water Clim Change*. <https://doi.org/10.2166/wcc.2021.093>
- Dutta D, Kundu A, Patel NR, Saha SK, Siddiqui AR (2015) Assessment of agricultural drought in Rajasthan (India) using remote sensing derived Vegetation Condition Index (VCI) and Standardized Precipitation Index (SPI). *Egypt J Remote Sens Space Sci* 18(1):53–63. <https://doi.org/10.1016/j.ejrs.2015.03.006>
- Farahmand A, AghaKouchak A (2015) A generalized framework for deriving nonparametric standardized drought indicators. *Adv Water Resour* 76:140–214. <https://doi.org/10.1016/j.advwatres.2014.11.012>
- Ganguli P, Reddy MJ (2013) Probabilistic assessment of flood risks using trivariate copulas. *Theor Appl Climatol* 111(1–2):341–360. <https://doi.org/10.1007/s00704-012-0664-4>
- Genest C, Favre AC, B eliveau J, Jacques C (2007) Metaelliptical copulas and their use in frequency analysis of multivariate hydrological data. *Water Resour Res* 43(9). <https://doi.org/10.1029/2006WR005275>
- Genest C, R emillard B, Beaudoin D (2009) Goodness-of-fit tests for copulas: a review and a power study. *Insur Math Econ* 44(2):199–213. <https://doi.org/10.1016/j.insmatheco.2007.10.005>
- Grinsted A, Moore JC, Jevrejeva S (2004) Application of the cross wavelet transform and wavelet coherence to geophysical time series. *Nonlinear Process Geophys* 11(5/6):561–566. <https://doi.org/10.5194/npg-11-561-2004>
- Guo Y, Huang S, Huang Q, Wang H, Wang L, Fang W (2019) Copulas-based bivariate socioeconomic drought dynamic risk assessment in a changing environment. *J Hydrol* 575:1052–1064. <https://doi.org/10.1016/j.jhydrol.2019.06.010>
- Gupta V, Kumar JM, Singh VP (2020) Multivariate modeling of projected drought frequency and hazard over India. *J Hydrol Eng* 25(4):04020003. [https://doi.org/10.1061/\(ASCE\)HE.1943-5584.0001893](https://doi.org/10.1061/(ASCE)HE.1943-5584.0001893)
- Hamed KH, Rao AR (1998) A modified Mann-Kendall trend test for autocorrelated data. *J Hydrol* 204(1–4):182–196. [https://doi.org/10.1016/s0022-1694\(97\)00125-x](https://doi.org/10.1016/s0022-1694(97)00125-x)
- Hao Z, AghaKouchak A (2013) A non-parametric multivariate multi-index drought monitoring framework. *Sp. Issue Adv Drought Monitoring*. *Am Met Soc* 15:89–101. <https://doi.org/10.1175/jhm-d-12-0160.1>
- Hao Z, Hao F, Singh VP, Zhang X (2018) Quantifying the relationship between compound dry and hot events and El Ni no–southern Oscillation (ENSO) at the global scale. *J Hydrol* 567:332–338. <https://doi.org/10.1016/j.jhydrol.2018.10.022>
- Harris IPDJ, Jones PD, Osborn TJ, Lister DH (2014) Updated high-resolution grids of monthly climatic observations—the CRU TS3.10 Dataset. *Int J Climatol* 34(3):623–642. <https://doi.org/10.1002/joc.3711>
- Himayoun D, Roshni T (2019) Spatio-temporal variation of drought characteristics, water resource availability and the relation of drought with large scale climate indices: a case study of Jhelum basin, India. *Quatern Int* 525:140–150. <https://doi.org/10.1016/j.quaint.2019.07.018>
- Huang S, Huang Q, Chang J, Zhu Y, Leng G, Xing L (2015) Drought structure based on a nonparametric multivariate standardized drought index across the Yellow River basin, China. *J Hydrol* 530:127–136. <https://doi.org/10.1016/j.jhydrol.2015.09.042>
- Huang S, Huang Q, Leng G, Liu S (2016) A nonparametric multivariate standardized drought index for characterizing socioeconomic drought: a case study in the Heihe River Basin. *J Hydrol* 542:875–883. <https://doi.org/10.1016/j.jhydrol.2016.09.059>
- Jha S, Das J, Goyal MK (2021) Low frequency global-scale modes and its influence on rainfall extremes over India: nonstationary and

- uncertainty analysis. *Int J Climatol* 41(3):1873–1888. <https://doi.org/10.1002/joc.6935>
- Joshi N, Gupta D, Suryavanshi S, Adamowski J, Madramootoo CA (2016) Analysis of trends and dominant periodicities in drought variables in India: a wavelet transform based approach. *Atmos Res* 1822:00–220. <https://doi.org/10.1016/j.atmosres.2016.07.030>
- Kao SC, Govindaraju RS (2010) A copula-based joint deficit index for droughts. *J Hydrol* 380(1–2):121–134. <https://doi.org/10.1016/j.jhydrol.2009.10.029>
- Keyantash JA, Dracup JA (2004) An aggregate drought index: assessing drought severity based on fluctuations in the hydrologic cycle and surface water storage. *Wat Resour Res* 40(9). <https://doi.org/10.1029/2003WR002610>
- Kim G, Silvapulle MJ, Silvapulle P (2007) Comparison of semiparametric and parametric methods for estimating copulas. *Comput Stat Data An* 51(6):2836–2850. <https://doi.org/10.1016/j.csda.2006.10.009>
- Krishnan R, Sabin TP, Madhura RK, Vellore RK, Mujumdar M, Sanjay J, Rajeevan M (2019) Non-monsoonal precipitation response over the Western Himalayas to climate change. *Clim Dyn* 52(8):4091–4109. <https://doi.org/10.1007/s00382-018-4357-2>
- Kumar KN, Rajeevan M, Pai DS, Srivastava AK, Preethi B (2013) On the observed variability of monsoon droughts over India. *Weather Clim Extremes* 1:42–50. <https://doi.org/10.1016/j.wace.2013.07.006>
- Kumar KS, Anand Raj P, Sreelatha K, Bisht DS, Sridhar V (2021a) Monthly and seasonal drought characterization using GRACE-based groundwater drought index and its link to teleconnections across south Indian river basins. *Climate* 9(4):56. <https://doi.org/10.3390/cli9040056>
- Kumar KS, Rathnam EV, Sridhar V (2021b) Tracking seasonal and monthly drought with GRACE-based terrestrial water storage assessments over major river basins in South India. *Sci Total Environ* 763:142994. <https://doi.org/10.1016/j.scitotenv.2020.142994>
- Kumar N, Poonia V, Gupta BB, Goyal MK (2021c) A novel framework for risk assessment and resilience of critical infrastructure towards climate change. *Technol Forecast Soc Change* 165:120532. <https://doi.org/10.1016/j.techfore.2020.120532>
- Liu S, Zhang J, Wang N, Wei N (2020) Large-scale linkages of socioeconomic drought with climate variability and its evolution characteristics in Northwest China. *Adv in Meteorol* 2020. <https://doi.org/10.1155/2020/2814539>
- Ma M, Ren L, Yuan F, Jiang S, Liu Y, Kong H, Gong L (2014) A new standardized Palmer drought index for hydro-meteorological use. *Hydrol Process* 28(23):645–5661. <https://doi.org/10.1002/hyp.10063>
- Mckee TB, Doesken NJ, Kleist J (1993) The relationship of drought frequency and duration to time scale. In: *Proceedings of the Eighth Conference on Applied Climatology*. American Meteorological Society pp. 179–184
- Mishra AK, Singh VP (2009) Analysis of drought severity-area-frequency curves using a general circulation model and scenario uncertainty. *J Geophys Res-Atmos* 114(D6). <https://doi.org/10.1029/2008JD010986>
- Mishra AK, Singh VP (2010) A review of drought concepts. *J Hydrol* 391(1–2):202–216. <https://doi.org/10.1016/j.jhydrol.2010.07.012>
- Mishra V, Aadhar S, Asoka A, Pai S, Kumar R (2016) On the frequency of the 2015 monsoon season drought in the Indo-Gangetic Plain. *Geophys Res Lett* 43(23):12–102. <https://doi.org/10.1002/2016GL071407>
- Mishra V, Shah R, Thrasher B (2014) Soil moisture droughts under the retrospective and projected climate in India. *J Hydrometeorol* 15(6):2267–2292. <https://doi.org/10.1175/JHM-D-13-0177.1>
- Nelsen RB (2006) *An introduction to copulas*. Springer, New York
- Nguyen DD, Jayakumar KV (2018) Assessing the copula selection for bivariate frequency analysis based on the tail dependence test. *J Earth Syst Sci* 127(7):92. <https://doi.org/10.1007/s12040-018-0994-4>
- Pathak AA, Dodamani BM (2020) Comparison of meteorological drought indices for different climatic regions of an Indian river basin. *Asia-Pac J Atmospheric Sci* 56(4):563–576. <https://doi.org/10.1007/s13143-019-00162-5>
- Poonia V, Jha S, Goyal MK (2021) Copula based analysis of meteorological, hydrological and agricultural drought characteristics across Indian river basins. *Int J Climatol*. <https://doi.org/10.1002/joc.7091>
- Rajsekhar D, Singh VP, Mishra AK (2015) Multivariate drought index: an information theory based approach for integrated drought assessment. *J Hydrol* 526:164–182. <https://doi.org/10.1016/j.jhydrol.2014.11.031>
- Salvadori G, Durante F, De Michele C (2013) Multivariate return period calculation via survival functions. *Water Resour Res* 49(4):2308–2311. <https://doi.org/10.1002/wrcr.20204>
- Shah D, Mishra V (2020) Drought onset and termination in India. *J Geophys Res Atmos* 125(15):e2020JD032871. <https://doi.org/10.1029/2020JD032871>
- Shah D, Mishra V (2020) Integrated Drought Index (IDI) for drought monitoring and assessment in India. *Wat Resour Res* 56(2):e2019WR026284. <https://doi.org/10.1029/2019WR026284>
- Shukla S, Wood AW (2008) Use of a standardized runoff index for characterizing hydrologic drought. *Geophys Res Lett* 35:L02405. <https://doi.org/10.1029/2007GL032487>
- Tan X, Gan TY, Shao D (2016) Wavelet analysis of precipitation extremes over Canadian ecoregions and teleconnections to large-scale climate anomalies. *J Geophys Res Atmos* 121(24):14–469. <https://doi.org/10.1002/2016jd025533>
- Tsakiris G, Pangalou D, Vangelis H (2007) Regional drought assessment based on the Reconnaissance Drought Index (RDI). *Water Resour Manag* 21(5):821–833. <https://doi.org/10.1007/s11269-006-9105-4>
- Vazifekkhah S, Kahya E (2019) Hydrological and agricultural droughts assessment in a semi-arid basin: inspecting the teleconnections of climate indices on a catchment scale. *Agric Water Manag* 217:413–425. <https://doi.org/10.1016/j.agwat.2019.02.034>
- Wang A, Lettenmaier DP, Sheffield J (2011) Soil moisture drought in China, 1950–2006. *J Clim* 24(13):3257–3271. <https://doi.org/10.1175/2011JCLI3733.1>
- Wang H, Kumar A (2015) Assessing the impact of ENSO on drought in the US Southwest with NCEP climate model simulations. *J Hydrol* 526:30–41. <https://doi.org/10.1016/j.jhydrol.2014.12.012>
- Won J, Choi J, Lee O, Kim S (2020) Copula-based Joint Drought Index using SPI and EDDI and its application to climate change. *Sci Total Environ* 744:140701. <https://doi.org/10.1016/j.scitotenv.2020.140701>

- Yevjevich VM (1967) Objective approach to definitions and investigations of continental hydrologic droughts, An (Doctoral dissertation. Colorado State University, Libraries)
- Zarch MAA, Sivakumar B, Sharma A (2015) Droughts in a warming climate: a global assessment of Standardized Precipitation Index (SPI) and Reconnaissance Drought Index (RDI). *J Hydrol* 526:183–195. <https://doi.org/10.1016/j.jhydrol.2014.09.071>
- Zhang H, Wu C, Yeh PJF, Hu BX (2020) Global pattern of short-term concurrent hot and dry extremes and its relationship to large-scale climate indices. *Int J Climatol* 40(14):5906–5924. <https://doi.org/10.1002/joc.6555>

Publisher's Note Springer Nature remains neutral with regard to jurisdictional claims in published maps and institutional affiliations.